RESOLVING THE ERA OF RIVER-FORMING CLIMATES ON MARS. E. S. Kite[1,2], A. Lucas[3], J.C. Armstrong[4], O. Aharonson[5], and M.P. Lamb[6]. [1]Princeton. [2]University of Chicago (kite@uchicago.edu). [3]Université Paris-Diderot. [4]Weber State University. [5]Weizmann Institute. [6]Caltech.

Introduction: River deposits record constraints that are sorely needed for Early Mars climate models. Although there is agreement that atmospheric precipitation (rain or snow/ice melt) was the water source for many of the rivers and streams of Early Mars [1-3], environmental scenarios for precipitation-fed runoff on Early Mars vary widely [4-9]. Lack of convergence in our understanding of what allowed rain or snowmelt on Early Mars is not the result of any lack of model sophistication; rather, what is currently in short supply are paleo-environmental proxies (ideally, time series) to constrain the models. Stratigraphic records of orbiter-resolved river deposits hold particular promise because rain or snowmelt must exceed infiltration plus evaporation to allow sediment transport by rivers. River deposits record climate events on Earth through changes in fluvial sediment volumes, channel dimensions, and channel-deposit architecture [10-12]. Therefore, river deposits could constrain the number, magnitudes, and durations of the wettest (and presumably most habitable) climates in Mars history. We are recovering an analogous fluvial record on Mars by measuring paleohydraulic proxies versus stratigraphic elevation in the >10^5 km^2 Aeolis Dorsa basin (10° E of Gale crater), noted for exceptional preservation of river and stream deposits [13-16]. The river deposits are eroding out of mappable rock units (Figure 1), and thus provide time-resolved climate constraints (river valleys provide time-integrated constraints). The range of river-deposit styles, the high frequency of interbedded impact craters, and evidence for major erosional episodes interspersed with deposition all suggest that Aeolis Dorsa's time series of constraints on climate is unusually long and complete [16, 17].

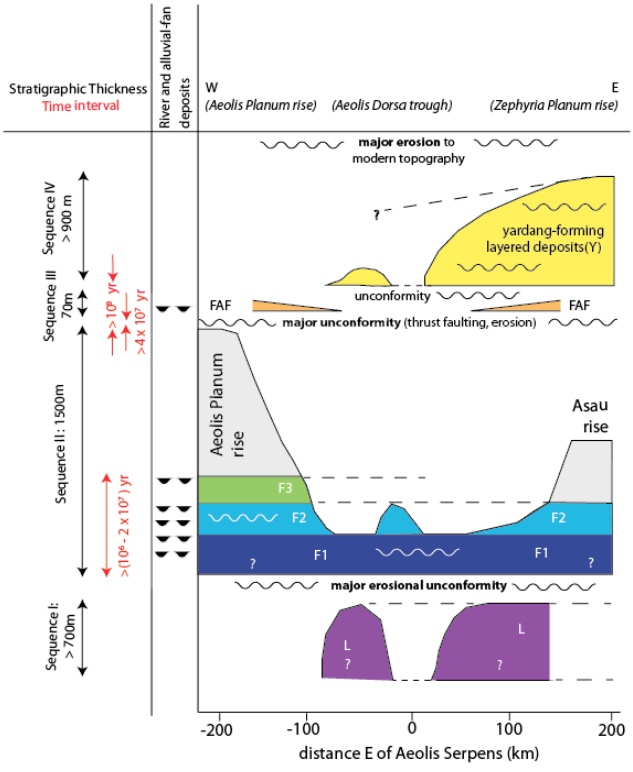

Fig. 1. Basin-scale stratigraphic framework showing context for river and alluvial-fan deposits. This study focuses on upper F1 through lower F3.

Approach: Paleodischarge is constrained by channel width and meander wavelength [13]; minimum runoff duration is found by dividing river-deposit volume by sediment flux (e.g. [18]); intermittency during a wet event is constrained by dividing the duration of runoff by the duration of sediment accumulation [16]; and the number of wet events is greater than or equal to the number of regionally correlatable fluvial packages. Our goal is to condense 3D paleohydraulic information in Aeolis Dorsa onto a single dimension - that of stratigraphy. However, basinwide postdepositional deformation [14] and large-scale unconformities complicate the use of elevation as a proxy for relative time across the basin. Therefore, we (1) identify large-scale unconformities, and thus place rocks in relative time order (Fig. 1); (2) krige between mapped contacts to define structure contours; (3) document all paleohydraulic proxies [19], tagging each measurement with its stratigraphic distance from adjacent contacts; and (4) isolate statistically distinct paleohydraulic facies.

Retrieval of climate change proxy data: example of HiRISE-scale results. River dimensions change coherently with stratigraphic position, suggesting wet-dry cycles at both long and short timescales superimposed on an overall drying-upwards trend.

As an example of paleohydraulic evidence consistent with a climate transition, a survey of 376 channel banks spanning 2 HiRISE DTMs and 250m of stratigraphy straddling the F1/F2 contact (Fig. 1) shows that channel width decreases from a mean of 31 m for stratigraphic levels below the interpolated F1/F2 contact to a mean of 21m more than 20m above the contact, a significant decline (Fig. 2). Changes in meander wavelength (measured using the method of [20]) are broadly correlative. Where channel width and meander wavelength can be measured at the same point (n = 44), width/wavelength ratios are usually consistent

with preservation of the original channel width as a channel deposit.

Assuming constant drainage density and drainage area, these paleohydraulic changes correspond to a twofold reduction in peak runoff production during the ≳(1-20) Myr duration of deposition (obtained from the frequency of craters interbedded with the river deposits; [16]). Based on theory, slow deposition rate, and the observation of small-scale cut-and-fill cycles, this is unlikely to have been a steady decline (models suggest that peak runoff corresponded to orbital optima and/or volcanic/impact transients). Because these rocks are part of a wind-eroded sedimentary basin in which original watersheds are not well constrained, we cannot rule out an alternative hypothesis in which catchment area changed with time. Atmospheric pressure during the time of the rivers probably did not stably exceed 0.9±0.1 bar [19]; these relatively low pressures are consistent with transient melting of ice or snow [19].

Using an additional HiRISE DTM, we have found that the narrowing-upwards and tightening-upwards of river channels shown in Fig. 2 is also found in lithostratigraphically-correlative rocks 80km further East within Aeolis Dorsa (number of measurements: n_λ = 69, n_w = 126). At the conference we will present extensions of our paleohydraulic measurements to higher (and lower) levels in the stratigraphic framework; these levels appear to record additional swings in climate (Fig. 1).

Acknowledgements: We thank D. Burr, L. Carter, L. Kerber, R. Jacobsen, B. Ehlmann, N. Finnegan, J. Stock, R. Irwin, G. Kocurek, R. Heermance, P. Olsen, K. Stack, R. DiBiase, A. Limaye, J. Scheingross, W. Fischer, K. Lewis, F. Simons, O. Bialik, and B. Hynek for useful suggestions. We thank R. Beyer, S. Mattson, A. Fennema, A. Howington-Kraus, and especially C. Phillips for help with DTM generation.

References: [1] Malin et al. (2010), *Mars J.* 4, 1. [2] Mangold et al. (2004), *Nature* 305, 78. [3] Irwin et al. (2005), *Geology* 33, 489. [4] Haberle et al. (2012), *LPSC* 43, 1665. [5] Kite et al. (2013), *Icarus* 223, 181. [6] Mischna et al. (2013), *JGR* 118, 560. [7] Toon et al. (2010), *AREPS* 38, 303. [8] Urata & Toon (2013), *Icarus* 226, 229. [9] Wordsworth et al. (2013), *Icarus* 222, 1. [10] Foreman et al. (2012), *Nature* 491, 92. [11] Amundson et al. (2012), *GSA-Bull.* 124, 1048. [12] Ward et al. (2000), *Science* 289, 1740. [13] Burr et al. (2010), *JGR* 115, E07011. [14] Lefort et al. (2012), *JGR* 117, E03007. [15] Williams et al. 2013, *Icarus* 225, 308. [16] Kite et al. (2013), *Icarus* 225, 850. [17] Kite et al. (2014), *Nature Geosci.*, doi:10.1038/ngeo2137. [18] Jerolmack et al. (2004), *GRL* 31, L21701. [19] Hajek & Wolinsky (2012), *Sed. Geol.* 257, 1. [20] Howard & Hemberger (1990), *Geomorphology* 4, 161.

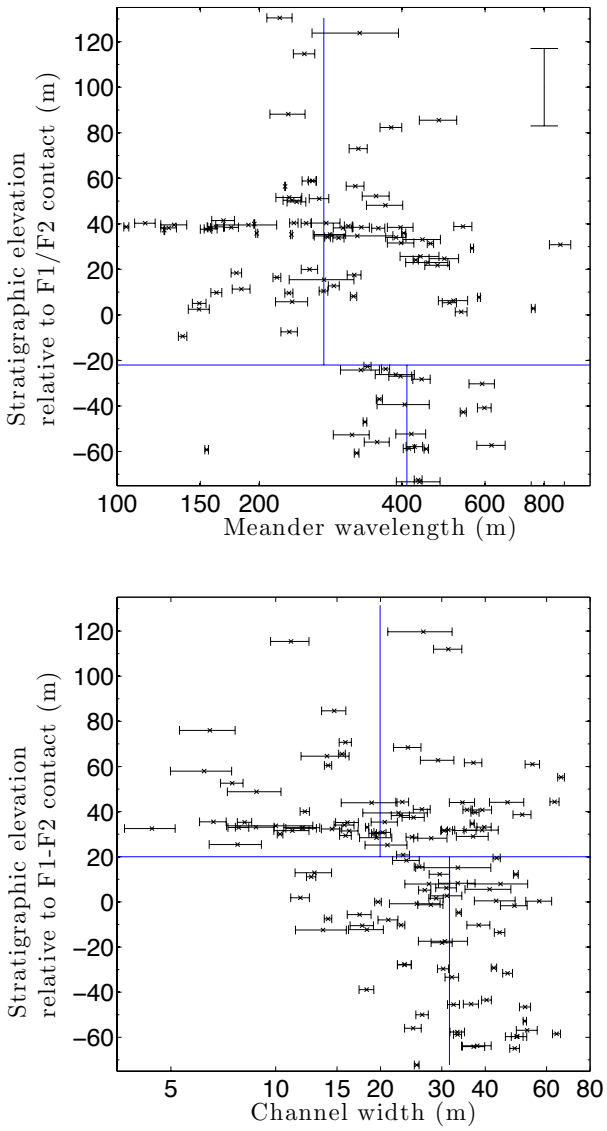

Fig. 2. Evidence for a drying-upwards sequence recorded by tightening-upwards (top panel) and narrowing (lower panel) of sinuous river channels in Aeolis Dorsa. n_λ = 102, n_w = 188. Best-fitting breakpoints in the nominal data are shown by horizontal lines. Vertical lines are mean values. Horizontal error bars correspond to standard deviation in independent re-tracings of meanders (top panel) and to width of individual channels (bottom panel). Typical stratigraphic error is shown by error bar in upper right of top panel.